Synthesis and characterization of Cu_2O thin films obtained from a CO_2-N_2 plasma mixture

M. C. González[a], V. H. Castrejon[a], P.G. Reyes[b], A.Gómez[b], H. Martinez[c], J. Vergara[d] and C. Torres[d]

[a]*TecNM/Tecnológico de Estudios Superiores de Jocotitlán (TESJo), Jocotitlán, Estado de México, México,*
[b]*Laboratorio de Física Avanzada, Facultad de Ciencias, Universidad Autonoma del Estado de México, 50200, México,*
[c]*Laboratorio de Espectroscopía, Instituto de Ciencias Físicas,*
Universidad Nacional Autonoma de México, Morelos 62210, México,
[d]*Laboratorio de Análisis y Sustentabilidad Ambiental, Escuela de Estudios Superiores de Xalostoc,*
Universidad Autonoma del Estado de Morelos, Morelos, 62717, México.

Received 11 January 2025; accepted 2 June 2025

In this study, a CO_2- N_2 plasma mixture was used to synthesize Cu_2O thin-films oxides metallics in a pulsed sputtering system. The plasma was generated using a percentage of 80% CO_2-20% N_2 between two copper (Cu) electrodes. The Cu_2O obtained were characterized by Raman spectroscopy, with the intention of detecting the bonding structure of the deposited thin films, while scanning electron microscopy (SEM) and atomic force microscopy (AFM) were used to study the surface morphology of the thin film. Dispersion Analysis (EDS) was conducted to determine the stoichiometric equilibrium present in the sample and X-ray diffraction (XRD) was used with the intention of determine the phases presents and their crystallographic orientation of the Cu_2O. The plasma characterization was performed during the deposition process using optical emission spectroscopy (OES), and the influence of the deposition process parameters on the chemical fragmentation of species present in the plasma was determined. The Raman results confirm the presence of Cu_2O films, and SEM analysis showed an irregular surface on the Cu substrate, forming a non-homogeneous surface. The morphology observed through AFM indicated that the thin films grew as islands, corroborating the generation of amorphous structures grown on the Cu surface. EDS analysis confirmed the presence of only copper and oxygen in the sample and XRD shows only the distinctive diffraction peaks in Cu_2O, whereas OES spectra confirmed the dissociation of CO_2 within the plasma, allowing for the presence of oxides within it.

Keywords: Plasma; thin films; Cu_2O; Raman spectroscopy; SEM; AFM; EDS; XRD; OES.

DOI: https://doi.org/10.31349/RevMexFis.71.061001

1. Introduction

In recent years, the implementation of cuprous oxide (Cu_2O) in the synthesis and characterization of new materials has aroused great interest due to its various applications in the fields of spintronics [1–3], optoelectronics [4], nanoelectronics [5], photovoltaics [6], and photo-catalysis [7, 8]. The characteristics of these new materials allow them to be implemented in the fabrication of various devices [9,10]. The use of Cu_2O in optoelectronic devices has gained momentum because it is a semiconductor oxide with natural p-type conductivity. Among the large variety of semiconducting oxides, Cu_2O has a cubic structure where the Cu^+ ions occupy the central face and the O^{2-} ions form body-centered cubic structures, featuring a direct band structure with bandwidth of 2.1 eV [11], characteristics that can be approved for photovoltaic and optoelectronic applications. The interest generated around the structure of Cu_2O within the area of material science at a theoretical and experimental level lies in the fact that Cu_2O has a high absorption coefficient, in addition to the fact that its production is relatively economical, and it is non-toxic.

Some of the methods implemented to obtain Cu_2O are by means of electrode position [12], thermal oxidation [13], wet chemical synthesis [14], and pulsed laser deposition [15], methods that can be very expensive and difficult to achieve. In recent years, the use of physical deposition methods to obtain Cu_2O has been implemented because it is a low-cost method, with which good results can be obtained and which can control physical parameters (pressure, current, sputtering power, polarization voltage of the substrate and target materials). Within the physical methods used to obtain this phase, in which we can find uses of plasmas, the best-known method for the generation of this material using plasmas is known as sputtering [16, 17]. This work reports the results obtained in a CO_2-N_2 plasma mixture generated from a pulsed discharge using the simplest sputtering configuration at a pressure of 1 Torr, a current of 500 mA, and a frequency of 35 kHz. The discharge was generated between the two Cu electrodes separated at a distance of 30 mm for 60 minutes. The concentrations used to generate the mixture were 80% CO_2 and 20% N_2. The products obtained were analysed using Raman spectroscopy. The morphology was analysed by SEM and AFM; in addition, the concentration of each element was analysed via EDS, and OES was used with the intention of analysing the parameters of the plasma, such as the electron temperature (T_e) and the electron density (n_e), as well as the atomic reactions and major molecules within the plasma, for which the results corroborate the generation of thin films of Cu_2O metal oxides.

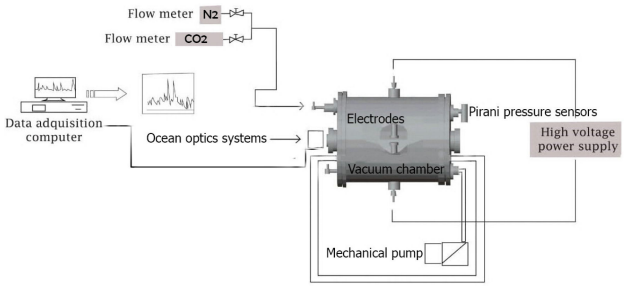

FIGURE 1. Experimental system.

2. Experimental setup

2.1. Plasma Source

A schematic illustration of the system used for the deposition thin films of oxides metallics is shown in Fig. 1 [18]. The system used was operated at a current of 500 mA, a voltage of 600 V, and frequency of 35 kHz with a power of 140 W between two electrodes, these parameters were generated from the Pinnacle Plus+ source, which delivered DC power in a pulsing configuration to enable the reactive sputtering of the plasma generated between two Cu electrodes (high-purity 99.9%), 5 cm in diameters and a thickness of 3 mm, placed in the center of the vacuum chamber with a separation of 30 mm. The pressure used to generate the plasma was a work pressure 1 Torr. Prior to deposition, the substrates were mechanically polished with fine-grit sandpaper (up to 1200 grit) and cleaned in acetone and ethanol each. During the deposition process, the substrate was not intentionally polarized, and its temperature was not actively controlled, remaining close to room temperature (≈ 25 °C) due to the power used (140 W) and the duration of the process (60 min.), which was determined through Pirani pressure sensors (MKS, model 103170027SH). In addition to this, the concentration of each gas within our system was regulated by means of a flowmeter (Matheson Tri. GasFM-1050). For OES measurements, an Ocean Optics FLAME-T-UV-vis spectrometer was used in a spectral range 200-1100 nm, with a resolution of 0.75 nm (FWHM), and the data were obtained with a step of 0.35 nm.

High-purity CO_2 (99.9%) and high-purity N_2 (99.9%) were both used as the sputtering ion source, which bombards the target. The ratio of the mixture was 80% CO_2 to 20% N_2 at a constant flux of 1.50 LPM. To generate plasma, the vacuum chamber was first evacuated with a mechanical pump until a base pressure of 2×10^{-2} Torr is reached; next, this was filled with an CO_2-N_2 mixture gas at 1 Torr, and discharge was generated by applying a pulsed current (500 mA at 600 V and 140 W) between two electrodes. The power of 140 W was selected based on previous experiments and earlier studies [18], which indicated that this power provides an optimal balance between plasma density and reactive species energy, allowing effective ionization and dissociation of CO_2 to produce oxygen atoms, as confirmed by OES analysis (Sec. 3.4). Powers lower than 100 W resulted in negligible deposition rates, while powers higher than 200 W generated rougher surfaces, likely due to excessive ion bombardment, according to preliminary SEM observations; this suggests that 140 W is adequate to generate reactive species without damaging the substrate.

The intention of generating the plasma at 1 Torr is because at these pressures there is a greater mobility of the ions for the formation of thin films of Cu_2O. This is due to the fact that there is a balance between the low gas density that reduces the collision frequency and the density sufficient to maintain a stable plasma. This combination allows the ions to move with less interference towards the substrate, resulting in a more efficient deposition and a better quality of the thin film.

Then, the CO_2-N_2 mixture gas is ionized and accelerated by the electric field produced by the electrodes, forming an energetic ion beam that provides both sputtering ions and reacting oxygen precursors. A Cu disk was used as a substrate for the growth of Cu_2O films, and the pulsed discharge was performed for 60 min. The deposition time of 60 min was chosen based on previous experiments, which showed that this duration allows the formation of films with a sufficient thickness ($\approx 100 - 200$ nm), where the amount of Cu deposited is enough to form a continuous and uniform film on the substrate. If the time were too short, the film could be very thin or incomplete. If the time were excessively long, unwanted layers could form or the quality of the copper oxide could be altered by effects such as over-oxidation. Therefore the 60 min. ensures that the Cu_2O deposition is carried out in a controlled manner, allowing the plasma to react properly with the copper and form the Cu_2O phase efficiently. CO_2 was used in our work as a source of oxygen atoms, with the intention of examining how this gas can be used in different ways because, in recent years, capture technologies have been developed to recycle, reform, or eradicate it. Within this, it can be seen that plasma technology is a good candidate for this particular issue because it is a clean and efficient technology, in addition to being easily accessible and economical. The plasma energy must be sufficient to brake the C=O bonds, thus generating CO and O as by-products in the system. These can be used because they can react with the surfaces that are in contact (in our case Cu) and form structures in the oxidation phase. Within our work, the O atoms are responsible for causing the Cu_2O phase since these are the ones that interact on the Cu surface. The intention of using the CO_2-N_2 mixture for film growth is because this mixture can provide a chemical environment which favors the formation of (Cu_2O). CO_2 acts as an oxygen source in the formation of oxides, while N_2 can stabilize reactive plasmas by reducing arcing and improving plasma homogeneity [19]. The use of CO_2 also allows for more precise control of the oxygen ratio in the plasma. This is crucial for Cu_2O growth, as the oxygen ratio directly affects the structural and electrical properties of the thin film. Too much or too little oxygen can lead to the formation of other compounds or to inferior

film quality, and the use of CO_2 and N_2 in the plasma can result in a more energy-efficient process compared to other gases, such as pure oxygen, which may require more energy to ionize. This can translate into lower operating costs and a more sustainable process.

2.2. Raman analysis

Raman spectra were obtained using micro-Raman, LabRam HR-800 system (Horiba Jobin Yvon, Kyoto, Japan) to determine the bond structure and microstructure of the thin films. Raman measurement were recorded using a He-Ne laser ($\lambda = 632$ nm), which was focused using a 50X lens. During the measurements, 60 recoded data were collected every 60 s.

2.3. SEM and EDS analysis

The morphology and elemental composition were studied using a Jeol IT-100 scanning electron microscope coupled to a Bruker X-Ray microprobe (Bruker Corporation, USA), operated in HV mode, with an accelerating voltage of 20 kV; a secondary electron signal was used to determined the type of thin film generated, in addition to the elements that were present in our analyzed sample.

2.4. AFM analysis

AFM (EasyScan 2 Flex AFM) was used to determine the thin-film morphology of the thin films generated and, thus, the surface roughness of the obtained films.

2.5. XRD analysis

X-ray diffraction (XRD) measurements were performed with an X-ray diffractometer (XDR, Bruker D8 Advanced) with a radiation of Cu Kα radiation of 1.5456 nm, a voltage of 40 kV, 30 mA to determine the phases presents and their crystallographic orientation of the Cu_2O thin films.

3. Result and discussion

In this work, thin-films of Cu_2O metal oxides were grown from a mixture of CO_2-N_2. The discharge generated by pulsed DC sputtering was carried out for 60 minutes, using CO_2, to take advantage of the O atoms coming from its dissociation. Thanks to the energy inside the plasma, the C=O bonds present can be broken down to generate O atoms, which can be used to interact with the Cu atoms that are detached from the target. This can lead to interaction, and the oxide phase of Cu can be generated. The thickness and morphology depend on the gas pressure and current used to generate the discharge, detaching Cu atoms from the surface and moving them toward the substrate by medium of the species involved to generate the plasma.

SEM studies were carried out on the substrate to observe the formation of adhered Cu_2O structures and, thus, corroborate the existence of data structure. The EDS analysis demonstrates the stoichiometry of Cu and O present within the analysed sample; the Raman spectroscopy analysis and the AFM analysis demonstrate that the structure formed of the Cu_2O obtained corroborate the results obtained by SEM, showing the topography, which shows a non-continuous surface on the substrate. This also shows the morphology of the Cu_2O thin films. The results obtained through OES demonstrate the dissociation of CO_2, finding O atoms, and showing that the plasma contains the necessary energy to break the chemical bond of CO_2, which is > 5.5 eV/molecules because it is the energy necessary to break said bond.

3.1. Raman spectroscopy

Raman spectra from 100 to 1200 cm^{-1} are shown in Fig. 2. The Raman spectrum shows the peaks corresponding to cuprous oxide (Cu_2O) structures [20], where the peaks observed at 79 cm^{-1} corresponded to a deformation band (δ) for Cu-Cu-O atoms, confirming the presence of metal-metal bonds; also, in the bond between Cu and O, the peaks 109 cm^{-1} (Γ_{12}^{-}) and 154 cm^{-1} ($\Gamma_{15}^{(1)}$(LO)) correspond to an inactive Raman mode and an infrared (IR) mode in perfect crystals of Cu_2O, respectively.

In the spectrum we can also observe an intense peak at 218 cm^{-1}, which is the second-order overtone $2\Gamma_{12}^{-}$. Additionally, a second-order overtone is detected at 308 cm^{-1} $2\Gamma_{15}^{(1)}$; a fourth-order overtone, $4\Gamma_{12}^{-}$ in 436 cm^{-1}; an allowed Raman mode, Γ_{25}^{+}, in 515 cm^{-1}. At 635 (TO) and 665 (LO) cm^{-1}, an allowed red mode is observed $\Gamma_{15}^{(2)}$, and a second-order combination $[\Gamma_{15}^{(1)} + \Gamma_{15}^{(2)}]$ at 820 cm^{-1}. Additionally, it should be noted that the predominance of the vibration mode in 218 cm^{-1} indicates the high structural quality of the synthesized sample [21–28], and the peak at 515 cm^{-1} is the only instance that is due to the Raman active mode (T_{2g}) [29–31].

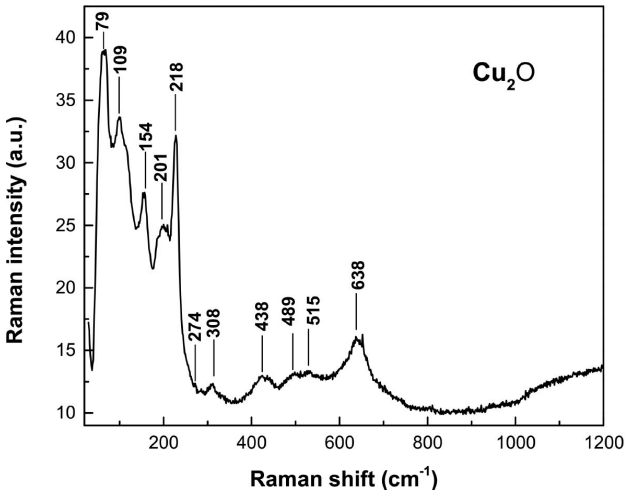

FIGURE 2. Raman spectra of the thin films of Cu_2O.

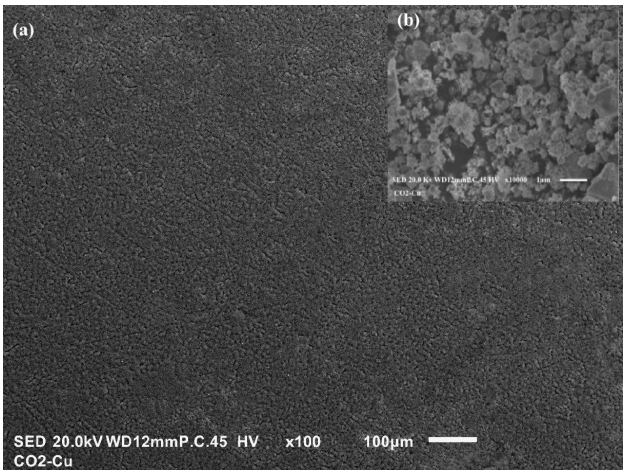

FIGURE 3. SEM micrographs of Cu_2O produced by CO_2-N_2 plasma, a) 100μm and b) 1μm.

3.2. SEM and EDS analysis

SEM images of the thin films of Cu_2O synthesized using a pulsed discharge are shown in Fig. 3. The results displayed that the synthesized Cu_2O is mainly constituted by a non-homogeneous film on the Cu surface: (a) as a consequence of the distribution of the grain on said surface, and (b) this can be explained by two factors: the energy, with which the plasma interacts with the surface of the target, is very high, owing to macro-particles that generate irregularities on the surface of the film and to the high internal stresses generated within the samples as a consequence of oxidation to create the cupric phase within our sample.

In the same way, we can say that the appearance of inhomogeneous surfaces is a consequence of the nucleation processes within the growth of the thin film, because it is considered a cluster-cluster aggregation, in which the random movement of many particles is involved (macro-particles).

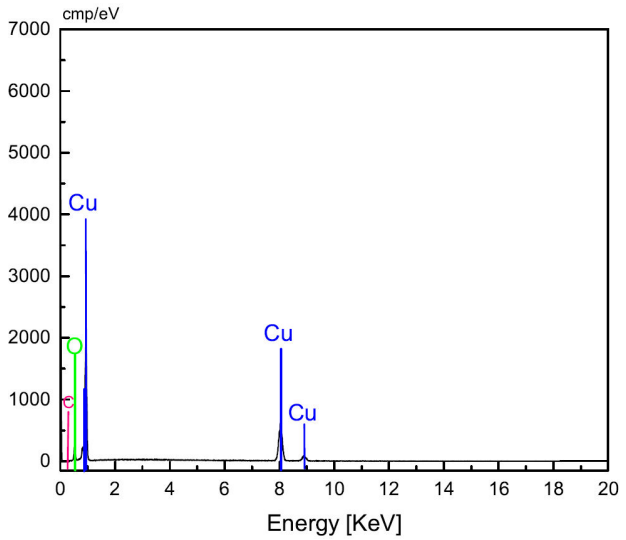

FIGURE 4. EDS spectra of the Cu_2O thin films with atomic ratio of 2:1.

TABLE I. Percentage of atoms in the analyzed sample.

Element	Atom [%] 100 μm	Atom [%] 1 μm
Cu	61.84	60.82
O	28.70	31.12
C	9.46	8.06

Particles stick together to form clusters, which continue to perform random walks until all particles are part of one single aggregate.

The EDS spectra of the Cu_2O thin-film samples (Fig. 4) clearly show the presence of peaks corresponding to the Cu and O elements. The observed atomic ratio of 2:1 between the Cu and O elements suggests the presence of Cu_2O in these films.

The carbon in the sample, as observed in the EDS spectrum, may be a product of the dissociation of CO_2, which is corroborated by the results obtained via OES. The percentage of atoms within the sample is presented in Table I, and according to the values obtained, we can corroborate the existence of the Cu_2O phase within the analyzed sample, which confirms the results obtained through Raman.

3.3. AFM Analysis

AFM images of the thin films grown over 60 min are shown in Fig. 5, where 2D and 3D images taken at 25 μm are presented, so that we could determine the morphology of the analyzed samples from two different profiles. In Figs 5a) and 5b) we can see a non-homogeneous surface, where, for both cases, island-type growth is observed instead of being a smooth continuous film. The grain growths observed in the Cu_2O most likely followed island-type growth, based on the shape and distribution of the grain for each film [32]; that is, the O atoms that reach the Cu surface can interact with them and diffuse, being absorbed in positions where the binding energy with the substrate is high. As atoms arrive, islands or agglomerations begin to form; subsequently, the larger agglomerates absorb the smaller groups, thus increasing their size.

As the agglomerates grow, they leave empty spaces between them, causing the growth to be like an island of the thin film, causing a non-homogeneous surface where the random distribution of the particles can be associated with the high surface mobility of the O particles that interact with the Cu surface with high kinetic energy. This is reduced by the Cu, which reduces the mean free path of the particles, reducing diffusion and favouring the formation of micro-particles and, as a consequence, the generation of inhomogeneous surfaces due to the appearance of peaks and valleys, which is in accordance with the obtained results. The grain size and roughness were calculated using statistical software for images (SPIP), obtaining a roughness of 18 nm and a grain size of 42.5 nm for the thin films grown at 1 Torr pressure.

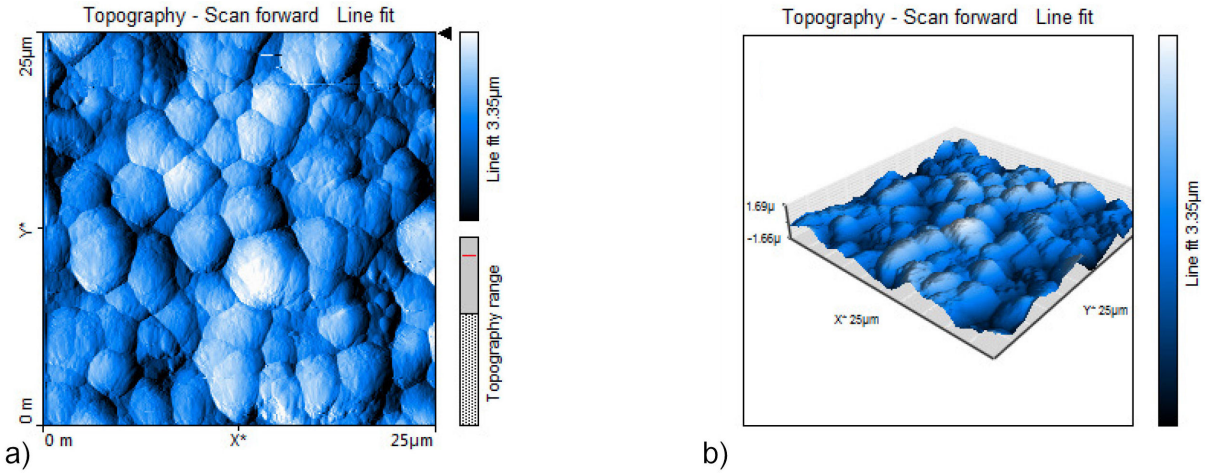

FIGURE 5. 2-D a) and 3-D b) images of Cu_2O thin films obtained by AFM.

3.4. XRD analysis

Figure 6 shows the X-ray diffraction (XRD) pattern of the Cu_2O thin film. The distinctive diffraction peaks at $2\theta \approx 30°$, 36°, 42°, 61° and 74° correspond to the (110), (111), (200), (220) and (311) planes of Cu_2O, respectively. The absence of CuO peaks (e.g., at $2\theta \approx 35.5°$ and 38.7°) indicates that the plasma conditions, likely influenced by reducing species such as CO, selectively favour the formation of Cu_2O over CuO.

The (111) peak at $2\theta \approx 36°$ shows the highest intensity, evidencing preferential texturing in the (111) direction. This orientation, promoted by the structural compatibility between the Cu substrate (face-centred cubic, FCC) and the Cu_2O, suggests a pseudo-epitaxial growth that can improve interfacial properties such as electrical conductivity and stability. Scherrer analysis estimates a nano-crystalline grain size of $\approx 16 - 17$ nm, consistent with the nano-structured morphology of the film. Peak broadening is attributed to inter-facial tensions arising from a $\approx 18\%$ lattice mismatch between Cu and Cu_2O, coupled with defects such as oxygen vacancies or composition gradients induced by substrate oxidation by reactive oxygen from CO_2 dissociation. The noisy background (≈ 400 counts) suggests slight amorphosity or incorporation of impurities, possibly nitrogen (from N_2) or carbon (from CO_2), at the film-substrate interface.

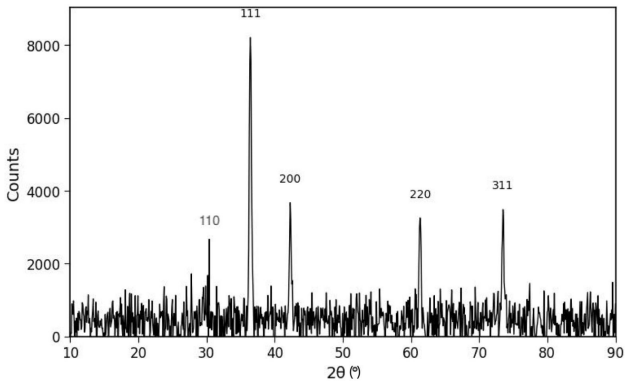

FIGURE 6. X-ray diffraction pattern of Cu_2O thin films deposited using CO_2-N_2 plasma.

3.5. OES analysis

The OES spectrum obtained from the discharge is show in Fig. 7. It is well known that atomic and molecular transitions emit photons with specific wavelengths and energies that correspond to the difference between the upper and lower energy levels involved in the transitions. The spectrum again shows the species of CO_2 (337, 375 nm) with transitions ($\nu_3 - \nu_{16}$) and ($\nu_{16} - \nu_{19}$) [33–35] , and CO with 451 and 483 nm characteristic peaks of the ($B^1\Sigma - A^1\Pi$) Angstrom band [36]. The emission of Swan band of C_2 ($500 - 520$ nm) arises from transitions between electronic states ($d^3\Pi_g - a^3\Pi_u$); O_2 had peaks 400 and 406 nm with transitions ($C^3\Delta_u - a^1\Delta_g$) and ($A^3\Sigma_u^+ - X^3\Sigma_g^-$), respectively [**?**, **?**] and O atomic at

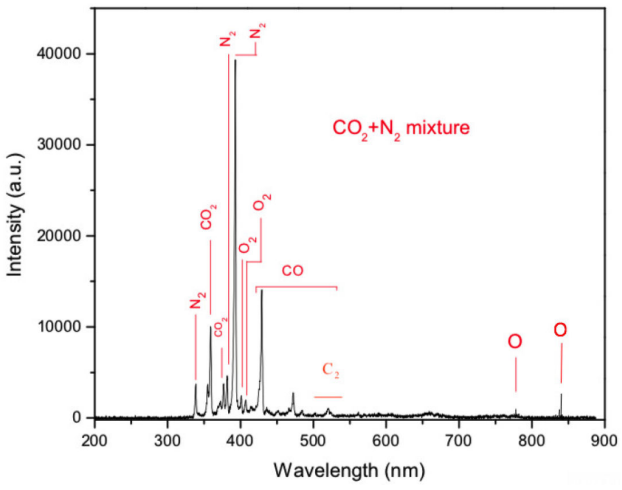

FIGURE 7. OES of CO_2-N_2, $I = 500$ mA, $V = 600$ V and 1.0 Torr.

at 777.1 ($^5S^0 - ^5P$) and 844 ($^3S^0 - ^3P$) nm, which can also be observed from the N_2 second positive system (SPS), ($C^3\Pi_u - B^3\Pi_g$) of N_2 at 337, 371 and 380 nm.

The species observed using OES within the plasma are formed because the electrons are accelerated by the electric field present within the plasma, producing ionization processes, excitation via electron impact, dissociation, and, in some cases, recombination processes. In the case of CO_2, electron-induced dissociation can also result in the formation of CO in its ground state ($^1\Sigma$) and O atoms in both the ground (^3P) and metastable (^1D) states [39], which can observed in Eq. (1). The excitation process of the dissociation products may additionally occur via the electrons impact, which may result in the corresponding excited states.

$$e + CO_2 \rightarrow CO(X\Sigma) + O(^3P^5, P) + e, \quad (1)$$

where, from the dissociation of CO_2 by means of (1), this can be followed by the recombination of the oxygen atoms, as observed in Eq. (2), which demonstrates the generation of oxygen atoms responsible for producing the oxidized phase of Cu.

$$O + O + M \rightarrow O_2 + M. \quad (2)$$

Something similar occurs for the molecules of N_2, which can be excited by means of electron impact

$$e + N_2(X) \rightarrow N_2(C) + e, \quad (3)$$

however, N_2 dissociation is weaker because of the higher dissociation energies of the N_2 compared with the CO_2 molecules, *i.e.*, 9.7 and 5.5 eV, respectively [19]. For this reason, only the SPS band characteristic of N_2 can be observed. An alternative form of CO_2 dissociation, which helps explain the presence of the C_2 swan band emission, is due to the following:

$$e + CO_2 \rightarrow C + O_2 + e. \quad (4)$$

The presence of C_2 can be taken as an indication of the formation of solid carbon, as presented in Eq. (4) due to the dissociation of CO_2, which also shown that C_2 initially nucleate in solid carbon groups [40]. On the other hand, within the discharge, there may be several possible reactions that are the result of the interaction of the electrons with the N_2 and CO_2 molecules. The appearance of the excited states of CO_2 and N_2 impacted by electrons; therefore, we consider that the most important reaction in plasma chemistry and for the generation of electric discharges in the CO_2-N_2 mixture is mainly related to electron impact (1) and (3). There may also be processes through recombination (2). In addition to this, in the same way that the discharge parameters were determined, such as the electron temperature (T_e) by the Boltzmann Plot method using the species coming from N_2 ($C^3\Pi_u - B^3\Pi_g$) [41, 42] and electron density (n_e) based on the Saha-Boltzmann method [43, 44], finding values of 7.8 (± 0.8) eV and $2.72 \pm 0.20 \times 10^{15}$ particles per cm^3 respectively, for the case of T_e. This suggests that the electrons in the high energy part of the electron energy distribution function produce the dissociation of CO_2 via the electron impact because the energy required to break the C=O bonds present in the molecule is at least 5.5 eV, and most of the electrons (low energy) participate in the excitation process of the species generated in the plasma. This leads to the formation of the CO_2, CO, and O and the appearance of the excited states of CO_2, in addition to the excited states of N_2. On the other hand, the result obtained for n_e promotes the electron impact excitation and ionization in the generated plasma, and, consequently, the transfer of energy from electrons to particles generated will lead to the formation of the excited states of CO_2 and N_2 and appearance of C_2 species. Furthermore, the values found for these parameters corroborate the results obtained via SEM and AFM for the morphology of the thin films because the value of T_e, likewise, suggests the expulsion of macro-particles; as a consequence, these are the causes of generating an irregular surface which is observed in these results.

4. Conclusions

In conclusion, thin films of metal oxides (Cu_2O) can be obtained from a mixture of CO_2-N_2 using DC pulsed sputtering technique (plasma technology). The films were obtained by taking advantage of the dissociation of CO_2 in O atoms that can interact with the Cu substrate to form Cu_2O. Raman analysis allowed us to determine the structure formed by the CO_2-N_2 plasma, confirming the existence of Cu_2O, because the Raman spectrum presents the characteristic peaks of Cu_2O, in which we can identify the peak at 79 cm^{-1} that corresponds to a deformation band (δ) for the atoms Cu-Cu-O atoms; this confirms the presence of metal-metal bonds and the bond between the Cu and the O. Furthermore, the predominance of the peak at 218 cm^{-1} indicates the high structural quality of the synthesized sample. Also, the appearance of the peak at 515 cm^{-1} is the only instance that is due to the Raman active mode (T_{2g}). The SEM and AFM results show the morphology of the grown structures. SEM analyses show irregular surface, which is expected due to the distribution of grain on the surface of the substrate, resulting in a non-continuous surface. AFM analysis showed island-type growth instead of a smooth continuous film. The grain growths of the Cu_2O most likely followed Volmer-Weber growth, based on the shape and distribution of the grain for each film. Furthermore, Volmer-Weber growth is typically the preferred growth mode for a normal metal film on a conductor substrate. The roughness value found is 18 nm, with a grain size of 42.5 nm. The EDS analysis confirmed the existence of Cu_2O as the spectrum only shows the peaks corresponding to Cu and O. The results provided by EDS suggest that the atomic ratio is 2:1 between the Cu and O elements, respectively. The XRD shows the distinctive diffraction peaks at $2\theta \approx 30°$, 36°, 42°, 61° and 74° corresponding to the (110), (111), (200), (220) and (311) planes of Cu_2O, respectively. Scherrer analysis estimates a nano-crystalline

grain size of 16-17 nm, which is consistent with the nanostructured morphology of the film. The dissociation of the CO_2 was verified using OES, finding the O atoms at 777 and 844 nm, which can interact with the Cu surface, forming the Cu_2O phase, which confirms the results obtained by means of Raman and EDS. Added to this, the values found for T_e and n_e (7.8 ± 0.8 ev and $2.72 \pm 0.28 \times 10^{15}$ particles per cm^3, respectively) corroborate the results obtained by SEM and AFM due to the energy with which the plasma interacts on the surface, producing the morphology of the grown film, which is non-homogeneous and with certain porosity, forming peaks and valleys.

1. Y. Zhang, F. Zhai and L. Yi,, Study of spin-polarized plasma driven by spin force in a two-dimensional quantum electron gas, *Physics Letters A* **46** (2016) 3908, https://doi.org/10.1016/j.physleta.2016.09.050
2. X. Hou, H. Sun, L. Liu, X. Jia and H. Liu, Unexpected large room-temperature ferromagnetism in porous Cu_2O thin films, *Journal of Magnetism and Magnetic Materials* **382** (2015) 20, https://doi.org/10.1016/j.jmmm.2015.01.041
3. S. E. Bogenrieder, J. Berner, A. K. Engstfeld, T. Jacob, First Principles Study on the Structural and Magnetic Properties of Low-Index Cu_2O and CuO Surfaces, *Chem.Rxiv* **1** (2024) https://doi.org/10.26434/chemrxiv-2024-29pkw
4. B. Rajesh Kumar, B. Hymavathi & T. Subba Rao, Structural and Optical Properties of Nanostructured Cu_2O Thin Films for Optoelectronic Devices, *Materials Today: Proceedings* **4** (2017) 3903, https://doi.org/10.1016/j.matpr.2017.02.289
5. S. Sharma, and J. Sharma, DFT study of electronic and optical properties of Cu_2O nanostructures, *AIP Conf. Proc.* **2093** (2019) 020032, https://doi.org/10.1063/1.5097101
6. T. S. Omelchenko, Y. Tolstova, Ha. A. Atwater, and N. S. Lewis, Excitonic Effects in Emerging Photovoltaic Materials: A Case Study in Cu_2O, *ACS Energy Letters* **2** (2017) 431, https://doi.org/10.1021/acsenergylett.6b00704
7. Y.A. Wu *et al*. Facet-dependent active sites of a single Cu_2O particle photocatalyst for CO_2 reduction to methanol, *Nat Energy* **4** (2019), 957, https://doi.org/10.1038/s41560-019-0490-3
8. Q. Su, C. Zuo, M. Liu, X. Tai, A Review on Cu_2O-Based Composites in Photocatalysis: Synthesis, Modification, and Applications. *Molecules* **28** (2023) 5576, https://doi.org/10.3390/molecules28145576
9. R.P. Wijesundera, L.K.A.D.D.S. Gunawardhana, and W. Siripala, Electrodeposited Cu_2O homojunction solar cells: Fabrication of a cell of high short circuit photocurrent, *Solar Energy Materials and Solar Cells* **157** (2016) 881, https://doi.org/10.1016/j.solmat.2016.07.005
10. L. Chau-Kuang Liau, Y.-C. Lin, and Yong-Jie Peng, Fabrication Pathways of p-n Cu_2O Homojunction Films by Electrochemical Deposition Processing, *J. Phys. Chem. C.* **117** (2013) 26426, https://doi.org/10.1021/jp405715c
11. B. Balamurunga, B. R. Mehta, Optical and structural properties of nanocrystalline copper oxide thin films prepared by activated reactive evaporation, *Thin Solid Films* **396** (2001) https://doi.org/10.1016/S0040-6090(01)01216-0
12. M. Izaki *et al*., Electrochemically constructed p-Cu_2O/n-ZnO heterojunction diode for photovoltaic device, *J Phys. D.* **40** (2007) 3326, https://doi.org/10.1088/0022-3727/40/11/010.
13. Sumita Choudhary, J. V. N. Sarma, and Subhashis Gangopadhyay, Growth and characterization of single phase Cu_2O by thermal oxidation of thin copper films, *AIP Conference Proceedings* **1724** (2016) 020116, https://doi.org/10.1063/1.4945236
14. W. Wang W, Z. Liu, Y. Liu, C. Xu, C. Zheng and G. Wang, A simple wet-chemical synthesis and characterization of CuO nanorods, Appl. Phys. A *76* (2003) 417, https://doi.org/10.1007/s00339-002-1514-5
15. K. Amikura, T. Kimura, M. Hamada, N. Yokoyama, J. Miyazaki, and Y. Yamada, Copper oxide particles produced by laser ablation in water, *Appl. Surf. Sci* **254** (2008) 6976, https://doi.org/10.1016/j.apsusc.2008.05.091
16. Z. Weifeng, C. Yue, P. Xihong, Z. Kehua, L. Yingbin, and H. Zhigao, The Phase Evolution and Physical Properties of Binary Copper Oxide Thin Films Prepared by Reactive Magnetron Sputtering, *Materials* **11** (2018) 1253, https://doi.org/10.3390/ma11071253
17. S. Hernando, Salapare III, A. Juvy, L. Balbarona, C. Pierre, and B. Arnaud, Cupric Oxide Nanostructures from Plasma Surface Modification of Copper, *Biomimetics* **4** (2019), 42, https://doi.org/10.3390/biomimetics4020042
18. M. C. González *et al*., Synthesis and Characterization of CN Thin Films Produced by DC-Pulsed Sputtering in an CH_3CH_2OH-N_2 Atmosphere, *Advances in Science, Technology and Engineering Systems Journal* **7** (2022) 53, https://doi.org/10.25046/aj070106
19. T. Silva, N. Britum, T. Godfroid and R. Snyder, Optical characterization of a microwave pulsed discharge used for dissociation of CO_2, *Plasma Sources Sci. Technol.* **23** (2014) 025009, https://doi.org/10.1088/0963-0252/23/2/025009
20. L. Debbichi, M. C. Marco de Lucas, J. F. Pierson and P. Kruger, Vibrational Properties of CuO and Cu_4O_3 from First-Principles Calculations, and Raman and Infrared Spectroscopy, *J. Phys. Chem. C* **116** (2012) 10232, https://doi.org/10.1021/jp303096m
21. Z. Weifeng, C. Yue, P. Xihong, Z. Kehua, L. Yingbin, H. Zhigao, The Phase Evolution and Physical Properties of Binary Copper Oxide Thin Films Prepared by Reactive Magnetron

Sputtering, *Materials* **11** (2018) 1253, https://doi.org/10.3390/ma11071253

22. S. Wang *et al.*, Nanoscale-Precision Removal of Copper in Integrated Circuits Based on a Hybrid Process of Plasma Oxidation and Femtosecond Laser Ablation, *Micromachines* **12** (2021) 1188, https://doi.org/10.3390/mi12101188
23. M. Ohring, The Materials Science of Thin Films. *Academic.Press.Inc* (1992) p. 53.
24. C. Carabatos, Lattice Vibrations of Cu_2O at the Long Wave Limit. *Phys. Status Solidi b* (1970) https://doi.org/10.1002/pssb.19700370228
25. F. I. Kreingold, V.L. Makarov, Resonance Interaction between Ortho- and Para-Exciton Levels Due to Phonons in a Cuprous Oxide Crystal, *Luminescence of Crystals, Molecules, and Solutions. Springer, Boston, MA.*, (1973), https://doi.org/10.1007/978-1-4684-2043-2_63
26. P. F. Williams, S. P. S. Porto, Symmetry-Forbidden Resonant Raman Scattering in Cu_2O, *Physical Review B.* **8** (1973) 1782, https://doi.org/10.1103/PhysRevB.8.1782
27. A. Compaan, H. Z. Cummins, Raman Scattering, Luminescence, and Exciton-Phonon Coupling in Cu_2O, *Physical Review B.* **12** (1972) 4753, https://doi.org/10.1103/PhysRevB.6.4753
28. S. Perusquía, P. G. Reyes, M. C. González, A. Gómez, H. Martínez, and J. Vergara, Experimental Study of Ethanol and Helium Mixture Glow Discharge, *IEEE Transactions on Plasma Science* **47** (2019) 445, https://doi.org/10.1109/TPS.2018.2863716
29. K. Reimann, K. Syassen, Raman scattering and photoluminescence in Cu_2O under hydrostatic pressure, *Physical Review B.* **39**, (1989), https://doi.org/10.1103/PhysRevB.39.11113
30. A. Compaan, Surface damage effects on allowed and forbidden phonon raman scattering in cuprous oxide, *Solid State Communications*, **6** (1975) 263, https://doi.org/10.1016/0038-1098(75)90171-4
31. T. Sander *et al.*, Correlation of intrinsic point defects and the Raman modes of cuprous oxide, *Phys. Rev. B.* **90** (2014) 04523, https://doi.org/10.1103/PhysRevB.90.045203
32. M. Ohring, The Materials Science of Thin Films. Academic Press, (New Jersey. 1992).
33. K. Tomas and B. Annemie, Splitting of CO_2 by vibrational excitation in non-equilibrium plasmas: A reaction kinetics model, *Plasma Sources Sci. Technol.*, **23** (2014) 045004, https://doi.org/10.1088/0963-0252/23/4/045004
34. M. Kraus, W. Egli, K. Haffner, B. Eliasson, U. Kogelschatz, and A. Wokaun, Investigation of mechanistic aspects of the catalytic CO_2reforming of methane in a dielectric-barrier discharge using optical emission spectroscopy and kinetic modeling, *Phys. Chem. Chem. Phys.* **4** (2002) 668, https://doi.org/10.1039/B108040G
35. X. Tu, White head J. C., Plasma-catalytic dry reforming of methane in an atmospheric dielectric barrier discharge: Understanding the synergistic effect at low temperature, *Appl. Catal.* **125** (2012) 439, https://doi.org/10.1016/j.apcatb.2012.06.006
36. A. Kumar, P. Ann Lin, A. Xue, B. Hao, Y. Khin Yap and R. Mohan Sankaran, Formation of nanodiamonds at near-ambient conditions via microplasma dissociation of ethanol vapour, *Nature Communication* **4** (2013) 2618, https://doi.org/10.1038/ncomms3618
37. G. Garcia-Cosio, M. Calixto-Rodriguez, H. Martinez, Low-pressure plasma discharge of $Ar/N_2/CO_2$ ternary mixture. *Am. Phys. Soc.* **54** (2009).
38. X. Zhu, X. Gao, C. Zheng, Z. Wang, M. Ni, and X. Tu, Plasma-catalytic removal of a low concentration of acetone in humid conditions, *RSC Adv.* **4** (2014) 37796, https://doi.org/10.1039/C4RA05985A
39. Y. Babou, P. Riviere, M.Y. Perrin and A. Soufiani, Spectroscopic study of microwave plasma of CO_2 and CO_2-N_2 mixtures at atmospheric pressure, *Plasma Sources Sci. Technol.* **17** (2008) 045010, https://doi.org/10.1088/0963-0252/17/4/045010
40. S. Kameshima, K. Tamura, Y. Ishibashi, and T. Nozaki, Pulsed dry methane reforming in plasma-enhanced catalytic reaction. *Catal. Today* **256** (2015) 67, https://doi.org/10.1016/j.cattod.2015.05.011
41. T. Volker and I. B Gornushkin, Importance of physical units in the Boltzmann plot method, *J. Anal. At. Spectrom.* **37** (2022) 1972, https://doi.org/10.1039/D2JA00241H
42. J. J. Camacho, J M. L. Poyato, l. Diaz and M. Santos. Optical emission studies of nitrogen plasma generated by IR CO_2 laser pulses, *J. Phys. B: At. Mol. Opt. Phys.* **40**, (2007) 4573. https://doi.org/10.1007/s11090-011-9307-2
43. M. Kono, M. M. Skoric. Nonlinear Physics of Plasma, *Springer Series on Atomic, Optical, and Plasma Physics* **978-3-642-14693-0**, (2010) . https://doi.org/10.1007/978-3-642-14694-7
44. N. Zhang *et al.*, Electron Temperature and Density of the Plasma Measured by Optical Emission Spectroscopy in VLPPS Conditions, *Journal of Thermal Spray Technology* **20** (2011) 1321. https://doi.org/10.1007/s11666-011-9681-6